SOME OBSERVATIONS ON CREEP BUCKLING ANALYSIS

B. HAYMAN

Department of Engineering, University of Leicester, Leicester LE1 7RH, United Kingdom

SUMMARY

Analytical studies are made of some simple model structures which contain nonlinear viscoelastic elements representing the effects of elasticity and steady-state metallic creep. The models have been chosen by virtue of their elastic postbuckling behaviour: one type has the stable elastic postbuckling response typical of columns, while another has the unstable type of postbuckling exhibited, for example, by certain shell structures. The simplicity of the models enables exact large deflection calculations to be made for both instantaneous elastic and time-dependent creep conditions, thus permitting a ready demonstration of the phenomena encountered. Analyses of the more familiar small-deflection type are also performed for comparison. Effects of changing such parameters as the creep index n and load level P are readily examined, as is the dependence on the size of the initial imperfection which, by its growth, leads to creep buckling.

The large deflection analyses indicate that the creep behaviour of the structures studied is intimately connected with the elastic postbuckling behaviour. For example, true constant-load creep instability characterised by infinite deflection rate at finite (critical) time and finite displacement is seen to occur only with structures with unstable elastic postbuckling. (The column is outside this category.)

It is widely known that small deflection analyses of purely elastic structures predict the growth of infinitely large deflections as P approaches the elastic critical load P_e, regardless of the true postbuckling behaviour. Thus, at given load, safe estimates of deflections tend to be obtained for structures with stable postbuckling and unsafe estimates for those with unstable postbuckling. Corresponding features are observed in small deflection analyses of the models under creep conditions: if elastic postbuckling is stable the deflections after a given time are overestimated, but if elastic postbuckling is unstable they are underestimated, the critical time being also an unsafe estimate in this latter case. It is found that in either case the degree of approximation in the small deflection analysis is very small provided:

(a) n is somewhat greater than unity (as it generally is),
(b) the imperfection is not too large, and
(c) P is not too close to P_e.

The range of admissible imperfection sizes and load levels is smaller for structures with unstable postbuckling, but these two parameters would in any case be severely restricted in the design of a practical structure on account of imperfection sensitivity in the purely elastic behaviour. Thus a small deflection creep buckling analysis is likely to be adequate provided the requirements for safe elastic behaviour are met.

Some discussion is included of the effects of instantaneous plastic strains. A brief survey is made of possible methods of estimating the critical time using as far as possible information gained from analysis of the instantaneous response of the structure.

1. Introduction

During the past twenty years a substantial amount of work has been published on the buckling of structures subject to creep. Most of the earlier studies were concerned with the creep buckling of columns, but more recently attention has turned towards plate and shell problems.

Papers on column buckling, such as that by Hoff (1), used a two-flange idealisation and the material was assumed to undergo elastic and steady-state creep strains:

$$\varepsilon = \varepsilon_e + \varepsilon_c \tag{1}$$

where $$\varepsilon_e = \frac{\sigma}{E} \quad \text{and} \quad \dot{\varepsilon}_c = \left(\frac{\sigma}{\lambda}\right)^n . \tag{2), (3}$$

In some studies the elastic strains ε_e were ignored. The column was assumed to be initially slightly curved in the shape of a half sine-wave and the analysis indicated that this imperfection would grow such that both lateral displacement and displacement rate became infinite at a finite critical time t^*, provided $n > 1$. For $n = 1$ the lateral displacement was found to be an exponentially increasing function of time, implying an infinite critical time. This type of behaviour is also exhibited by a simple rigid link column model examined by Hult (2).

Later papers such as those by Hoff (3) and Patel (4) used the same type of analysis but accounted for instantaneous plastic strains and transient creep by adding a further term to eq. (1):

$$\varepsilon = \varepsilon_e + \varepsilon_p + \varepsilon_c \tag{4}$$

where $$\dot{\varepsilon}_p = \left(\frac{\sigma}{\mu}\right)^m \frac{\dot{\sigma}}{\mu} = \frac{1}{m+1}\frac{d}{dt}\left[\left(\frac{\sigma}{\mu}\right)^{m+1}\right] \tag{5}$$

when $|\sigma|$ is increasing; $\dot{\varepsilon}_p$ is zero when $|\sigma|$ is decreasing. Chapman et al (5) later produced a partly graphical procedure for dealing with more general plastic stress-strain relations. The results of these studies differ from those ignoring instantaneous plasticity in that they indicate that, when at the critical time t^* the displacement rate becomes infinite, the displacement itself is still finite. Furthermore, this critical displacement has a value dependent only on the parameters associated with the instantaneous response, and not on the creep constants λ and n.

Each of the studies so far described was based on the conventional type of bending analysis in which the curvature is taken as $\partial^2 w/\partial x^2$, where w is the lateral displacement and x the distance along the axis. This is usually referred to as a small deflection analysis: the approximation results from ignoring $\partial w/\partial x$ compared to unity.

More recently the ideas developed in the context of columns have been extended to plates and shells. Generally the plate or shell has been replaced by a "sandwich" idealisation, the creep law has been a generalisation to two-dimensional plane stress of eq. (3), instantaneous plasticity has been omitted and small deflection analyses have been used. Hoff analysed the creep buckling of compressed rectangular plates (6) and also the axisymmetric creep buckling of imperfect, long cylindrical shells under axial compression (7), finding that in both cases the displacement rates became infinite at infinite displacement. Fairly simple approximate formulae were obtained for the critical times for $n = 3$, these being infinite for $n = 1$. Samuelson (8) also considered the axisymmetric buckling of shorter cylindrical shells, choosing a numerical method of solution. In a later paper (9) he studied the buckling of axially and radially loaded cylinders with nonaxisymmetric imperfections and radial loads. In order to describe adequately the interaction between axisymmetric and nonaxisymmetric displacements he used a moderately large deflection computer analysis retaining nonlinear terms in the shell equations. Samuelson's results indicate a very marked sensitivity to nonaxisymmetric imperfections and loads which appears to be the counterpart of the imperfection sensitivity encountered in the elastic response of these shells.

This brief historical introduction to creep buckling analysis is by no means complete: further references are to be found in the recent review by Hoff (10). The purpose of this account has been to show certain features of the process of development: that small deflection theories have generally indicated finite critical times provided $n > 1$ and that these analyses suggest that creep buckling occurs at a finite critical displacement only if instantaneous plasticity is present: that in the analysis of compressed cylinders a moderately large deflection analysis has been considered necessary to describe the behaviour. The present paper attempts, by analysis of some simple structural models, to account for some of these features in simple terms and to draw some conclusions which may be of wider application. Instantaneous plasticity is ignored in the main analysis, section 3, but is discussed in section 4. However, it is first necessary to describe briefly the general features of the buckling of elastic structures.

2. Elastic Buckling

Detailed accounts of the buckling and postbuckling of elastic structures have been given, for example, by Croll and Walker (11) and by Thompson (12). Briefly, the stability of equilibrium of an elastic structure subjected to a conservative load P can be determined by reference to a graph of P against a suitably chosen measure of deflection δ. A transition from stable to unstable equilibrium is possible only at a critical point, which is in general either a limit point (at which the graph reaches a maximum value of load) or a bifurcation (at which two or more paths intersect) Confining attention to the latter group, the three most common types of load-deflection relation are shown in Fig. 1(a) to (c), in which stable equilibrium states are shown by full lines and unstable states by broken lines. With each of these the structure remains undeflected (or virtually so) and in stable equilibrium up to the bifurcation at the critical point C, with critical load P_e. For $P > P_e$ the undeflected state is unstable and the response of the structure depends on the nature of the postbuckling equilibrium path which crosses over at C. Fig. 1(a) shows a stable symmetric bifurcation, in which this path has zero slope at C itself but rises to either side, presenting displaced configurations of stable equilibrium at loads above P_e In practice this type of load-deflection graph is never actually achieved, and slight geometric deviations from the "perfect" bifurcating structure result in a smooth curve of the type marked "imperfect" The practical structure develops rather large deflections at loads near P_e but never actually becomes unstable. Fig. 1(b) shows the case when the postbuckling path drops away to either side of C, the unstable symmetric bifurcation. A practical structure then has a load-deflection graph which reaches a maximum, with consequent sudden failure, at a new critical load somewhat below P_e Sometimes the dependence of the actual critical load on the size of imperfection is quite strong. Fig. 1(c) shows an asymmetric bifurcation. The practical structure's behaviour now depends on whether the imperfections tend to push it in the stable direction ($\delta<0$) or the unstable ($\delta>0$). In the former case there is no collapse, but deflections may become large around $P=P_e$. In the latter there is a sudden failure at a new critical load which may be appreciably below P_e.

Fig. 1(a) to (c) represent the true behaviour of a number of structures under load. If any of these structures is analysed by a small deflection analysis of the type referred to in section 1, the behaviour predicted is that of Fig. 1(d). The critical bifurcation load P_e of the perfect structure is predicted correctly, but the postbuckled path appears horizontal, representing neutral equilibrium at $P=P_e$. An imperfect structure appears to develop infinite deflection as $P\to P_e$. The relationship between Fig. 1(a) and (d) is precisely that between the elastica theory for the buckling of a strut and the conventional treatment of the problem. In this example the difference becomes important only at quite large deflections, and the simple small-deflection theory overestimates the deflection at any given load. The inaccuracy is still on the safe side, though possibly rather larger, when a structure of type (c) has imperfections pushing it in the stable direction. However if the postbuckling is unstable, whether type (b) or type (c), the small deflection analysis is liable to be unsafe and in some cases seriously so.

3. The Models and their Behaviour

3.1. The First Link Model

The first link model examined is shown in Fig. 2(a). AB is a rigid rod pivoted at B and restrained by the spring AC. In studying the instantaneous response we take the spring as linear and perfectly elastic. Thompson (13) has examined this model's elastic response in detail. If AC has an unstretched length $R\sqrt{2}$ then AB is initially vertical and when loaded the system exhibits the asymmetric bifurcation of Fig. 1(c). The postbuckling path is stable for $\theta < 0$ and unstable for $\theta > 0$. If the spring is initially shorter than $R\sqrt{2}$ there is a bias to negative values of θ and the resulting "imperfect" system has the entirely stable behaviour described earlier. If the spring is too long the system becomes unstable with collapse occurring at a new critical load $P_e' < P_e$. If, for example, the spring is long by 0.2% then P_e' is about 10% below P_e It is useful to draw the locus of critical points obtained for systems with successively greater imperfection sizes: this is included in Fig. 2(b).

To examine the creep behaviour we replace the spring AC by an element whose material obeys eq. (1) to (3). We consider first the response when AC is initially longer than $R\sqrt{2}$ by an amount $R\sqrt{2}\varepsilon_i$, so that before any load is applied $\theta = \theta_i$ where $\theta_i > 0$. A constant load $P < P_e$ is now applied, and the response is shown in Fig. 2(b). There is an immediate increase of deflection to $\theta = \theta_o$, point X, followed by a time-dependent deflection due to creep, represented by the line of arrows. This line will be referred to here as the creep line. During this process the creep strain ε_c is gradually increasing; some change in the elastic strain ε_e also occurs as the changing geometry increases the tension in AC.

Now suppose there is a change of conditions at some time t at which the creep strain is ε_c. In the instantaneous response to this the creep strain cannot change, and so the system responds just as if it had been elastic with AC too long by $R\sqrt{2}$ $(\varepsilon_i+\varepsilon_c)$, i.e. with an increased imperfection. A complete elastic load-deflection graph may be drawn for this new imperfect structure, and it has a critical point which lies on the critical point locus already drawn. Thus at any stage of the creep process the instantaneous response of the system to any change of conditions will be determined by the elastic load-deflection curve with the appropriate imperfection $R\sqrt{2}(\varepsilon_i+\varepsilon_c)$ in AC. Now for this particular structure the elastic critical load of the imperfect system falls as the imperfection increases and it is clear that it must eventually be reduced to the value of the actual applied load P. This happens when the creep line meets the critical point locus, at point Y in Fig. 2(b). At this point the structure exhibits a critical point in its instantaneous behaviour and collapse follows.

By an exact analysis it is found that during the creep process XY the displacement rate $\dot{\theta}$ is given by

$$\dot{\theta} = \frac{\left[\frac{E}{\lambda} \cdot \frac{P}{P_e} \cdot \frac{1}{2} \tan\theta \sqrt{(1+\sin\theta)}\right]^n}{\frac{\partial}{\partial\theta}\left[\left(1-\frac{1}{2}\frac{P}{P_e}\tan\theta\right)\sqrt{(1+\sin\theta)}\right]} \tag{6}$$

Clearly $\dot{\theta} \to \infty$ when the denominator becomes zero. It is found that this condition is precisely the equation of the critical point locus, which confirms that collapse does indeed occur when the locus is reached. (We are ignoring inertia effects.) By use of this condition the critical deflection θ^* may be calculated for any given P. The critical deflection, being essentially a feature of the imperfect elastic behaviour, is independent of the creep constants λ and n.

Numerical integration of eq. (6) enables the displacement-time relation to be found. The critical time t^*, which is the time taken to reach the collapse condition, may be found by integrating between the limits θ_o and θ^* t^* depends on λ and n but is finite for all values of these constants.

Turning to the case when AC is initially short, so that ε_i, θ_i and θ_o are all negative, it is found that $\dot{\theta}$ never becomes infinite, indicating the absence of this type of creep buckling. With imperfections of this sign the elastic response is always stable so that the creeping structure cannot encounter an elastic critical point.

All of these results have been obtained using an analysis which completely describes the large deflection behaviour without any geometric simplifications. With both elastic and creep analyses it is possible to use instead a small deflection formulation. The approximation consists in expanding the trigonometric functions of θ as power series and ignoring high order terms. The elastic response indicated by such an analysis is just as in Fig. 1(d). For creep at constant P, the analysis suggests that, for $\theta > 0$,

$$\dot{\theta} = \frac{\left[\frac{E}{\lambda} \cdot \frac{P}{P_e} \quad \frac{1}{2}\theta\right]^n}{\frac{1}{2}\left(1 - \frac{P}{P_e}\right)} \tag{7}$$

It is seen that $\dot{\theta}$ cannot become infinite at finite θ unless $P = P_e$. This is because the analysis fails to show a falling critical point locus. However, $\dot{\theta} \to \infty$ as $\theta \to \infty$. An explicit expression is found for the apparent critical time:

$$t^* = \frac{1}{n-1}\left[\frac{\lambda}{E}\left(\frac{1 - P/P_e}{P/P_e}\right)\right]^n \left(\frac{2}{\theta_i}\right)^{n-1} \tag{8}$$

where $\theta_i = 2\varepsilon_i$. This is finite and positive only if $n > 1$. These results are similar in nature to those of the treatments of creep buckling (1,2,6,7) which also ignored plastic strains.

If $\theta_i < 0$ the behaviour predicted by the small deflection analysis is just the same as for $\theta_i > 0$: the asymmetry of the problem has been lost.

To permit a comparison of the two methods of analysis, eq. (6) and (7) have both been integrated, with the aid of a computer, to give the full displacement-time relations for a large number of conditions, and the critical deflections and critical times have also been computed where they exist. Fig. 3 shows the displacement-time curves for $n = 1$, $P/P_e = 0.9$ and $\theta_i = \pm 0.001$ radian (corresponding to $\varepsilon_i = \pm 0.0005$): these are cases in which the two analyses produce quite different results.

The following conclusions are drawn from these analyses:

(i) For $\theta_i > 0$ (unstable elastic postbuckling), the true behaviour consists in buckling at finite θ^* and finite t^* for all values of n. A small deflection analysis suggests instead that $\dot{\theta} \to \infty$ as $\theta \to \infty$ and that t^* is finite and positive only if $n > 1$. It also underestimates θ at all values of t.

(ii) For $\theta_i < 0$ (stable elastic postbuckling), the true behaviour is a steadily increasing deflection. A small deflection analysis suggests that $\dot{\theta} \to -\infty$ as $\theta \to -\infty$ with finite, positive t^* if $n > 1$. It overestimates θ at all t.

The degree of divergence between the analyses may be assessed using Table I, which shows some relevant quantities for $\theta_i > 0$. Columns 6 and 8 show the large and small deflection analysis predictions of the time taken for the structure to reach $\theta = 0.2$ radian; values in brackets indicate that buckling has already occurred. When $n = 1$ there are quite large differences in behaviour which are associated with the fact that the small deflection analysis fails to predict a finite t^*, and comparison of columns 6 and 8 is relevant here. The small deflection analysis nevertheless gives quite a good prediction of the displacement-time relation, even to such large deflections as 0.2 radian, provided neither θ_i or P/P_e is too large. If $P/P_e = 0.5$, then the discrepancy is rather noticeable for θ_i greater than about 0.01 radian, and is an order of magnitude when θ_i approaches 0.1 radian. If $P/P_e = 0.9$ the discrepancy is noticeable at very small imperfections indeed and the situation becomes very much worse as θ_i is increased. (When θ_i has a value of about 0.004 radian this load causes immediate elastic buckling, $t^* = 0$.) When $n = 3$ the differences are much smaller, though they are still quite appreciable if P/P_e is near unity or if θ_i is large. Computations with higher values of n have shown these trends to be continued.

We conclude that the discrepancies between large and small deflection analyses are small provided:

(a) n is somewhat greater than unity,

(b) the imperfection θ_i is not too large, and

(c) P is not too close to P_e.

Similar features are observed if $\theta_i < 0$, the deflections now being overestimated by the small deflection analysis. Conditions (a) to (c) will be discussed further in section 6

3.2 The Second Link Model

The second link model is shown in Fig. 4. It consists of a single rigid link EF restrained by a rotational spring whose material law corresponds to that of the spring AC of the first model. If the rod is initially vertical the elastic system exhibits the stable symmetric bifurcation of Fig. 1(a). If the spring is initially too long or too short, so that initially $\theta = \theta_i$, then the elastic response is entirely stable but with large deflections developing around $P = P_e$.

We consider a system with $\theta_i > 0$: the symmetry of the system ensures that identical behaviour will be observed if $\theta_i < 0$. If a constant load $P < P_e$ is applied and the material of the spring is allowed to creep, the displacement rate is given by

$$\dot{\theta} = \frac{\left[\frac{E}{\lambda} \cdot \frac{P}{P_e} \cdot \sin\theta\right]^n}{1 - \frac{P}{P_e}\cos\theta} \tag{9}$$

We note that $\dot{\theta}$ remains finite at all θ, whatever the value of n. This is similar to the behaviour of the first model when deflecting in the stable direction, and reflects the absence of any elastic critical points for the structure to encounter.

If a small deflection analysis is used, it is found that

$$\dot{\theta} = \frac{\left(\frac{E}{\lambda} \cdot \frac{P}{P_e}\,\theta\right)^n}{1 - P/P_e} \tag{10}$$

Thus $\dot{\theta} \to \infty$ as $\theta \to \infty$ at critical time t^*, where

$$t^* = \frac{1}{n-1}\left[\frac{\lambda}{E}\left(\frac{1 - P/P_e}{P/P_e}\right)\right]^n \left(\frac{1}{\theta_i}\right)^{n-1} \tag{11}$$

t^* is finite and positive provided $n > 1$. Eq. (10) and (11) are almost identical to the corresponding eq (7) and (8) for the first model.

Comparison of the displacement-time relations has been made for a number of cases, and the general features are much the same as for the first model deflecting in the stable direction. For the present model, with either sign of imperfection θ_i, a small deflection analysis overestimates the deflection at any time t Thus a design based on such an analysis is safe in all cases. Agreement between the two analyses is in general much closer for this model than for the first, but again the discrepancies may become appreciable if any of the conditions (a) to (c) of section 3.1 are violated.

3.3 Shanley Column Model

In order to represent more closely the creep buckling behaviour of compressed columns, plates and shells, in which buckling occurs as a result of bending rather than pure extension or compression of an element, the Shanley column model (Fig. 5) has also been examined. The two flange elements of the central cell are assumed to be of a material obeying eq. (1) to (3): instantaneous plastic strains are still ignored.

The instantaneous elastic response of the Shanley column is precisely as for the second link model, having a stable symmetric bifurcation similar to that of a continuous elastic column. Under creep conditions the behaviour is much the same as for the second link model, though stress reversal in one of the flanges makes the analysis more complicated. The large deflection analysis for $P < P_e$ shows that $\dot{\theta}$ never actually becomes infinite, since once again there are no elastic critical points for the creeping system to encounter, but $\dot{\theta}$

does become quite large at larger values of θ. The small deflection analysis, as usual, suggests that $\dot{\theta} \to \infty$ as $\theta \to \infty$ at a t^* which is finite provided $n > 1$. It is impossible to obtain a general, explicit expression for t^* valid for all n, but for n = 3

$$t^* = \frac{a}{3} \frac{(1 - P/P_e)}{\left(2a \frac{E}{\lambda} \cdot \frac{P}{P_e}\right)^n} \log_e \left(\frac{3 + x_o^2}{x_o^2}\right) \tag{12}$$

where $a = c^2/b\ell$, $x_o = \theta_o \ell/c$ and $\theta_o = \theta_i/(1-P/P_\varepsilon)$. Eq. (12) is very similar to the expressions obtained by Hoff (1,6,7) for the critical times of columns, plates and shells with n = 3. It is seen that t^* depends less heavily on the magnitude of the imperfection θ_i than the critical times of the first two models: this results in some way from the presence of bending effects in this problem. In almost all other respects the Shanley column model displays the same features as the second link model, and the differences between large and small deflection analyses seem to depend very little on the slenderness ratio.

4. Effects of Instantaneous Plastic Strains

We examine briefly the behaviour of two of the models when the material undergoes instantaneous plastic strains, eq. (4). No specific $\varepsilon_p - \sigma$ relation is assumed.

Referring to the first link model with $\theta_i > 0$, both instantaneous and creep analyses proceed just as before but the current tangent modulus E_t replaces the elastic modulus E. This is possible because the stress in AC increases monotonically with θ (up to $\theta = \pi/2$). Whereas previously creep buckling occurred when the elastic critical point locus was reached, it now happens when the locus of tangent modulus critical points is encountered. Since E_t becomes progressively smaller than E as the deflections increase and the stress in AC increases, this locus falls more steeply than the elastic critical point locus. Thus collapse occurs earlier than previously. The drop in E_t with increasing deflection also suggests that a system with $\theta_i < 0$ may encounter a tangent modulus critical point, although no <u>elastic</u> critical points exist in that region.

Analysis of the Shanley model is more complicated because one of the flanges unloads as the deflections proceed, and the reduced modulus E_r now governs the behaviour. As E_r decreases with increasing deflection in much the same way as E_t, the instantaneous response curves drop below the elastic curves, generating critical points at the appropriate reduced modulus critical loads. In this way a falling locus of reduced modulus critical points is generated which is analogous to the falling critical load locus of the first link model. Creep buckling, with $\dot{\theta} \to \infty$ at finite θ^* and finite t^*, is found to occur in this situation, in contrast to the behaviour in the absence of instantaneous plasticity.

Full comparison of large and small deflection analyses has not been undertaken for these two problems. However, it is apparent that even a small deflection analysis can predict a falling critical point locus when the tangent modulus or reduced modulus is used, and can therefore indicate buckling at finite θ^* and finite t^* (though the predicted values of these quantities may not be particularly accurate).

5. Approximate Estimates of Critical Time

We now turn attention to problems in which a large deflection computation of the critical time is so complex as to be impracticable, but a small deflection analysis is inadequate. Plastic strains will be ignored.

Consider the first link model with $\theta_i > 0$. The critical deflection θ^* may be found from the elastic critical point locus, a feature of the elastic response of the family of imperfect systems. This calculation may itself be quite complex, though Koiter's asymptotic method, as used by Thompson (12,13), may give a satisfactory estimate if P is fairly near to P_e Supposing that θ^* and θ_o have been found, we now wish to estimate the time which the system takes to get from θ_o to θ^* One possibility is to use the small deflection displacement-time relation between these limits, and if θ_o and θ^* have been determined exactly this value of t^* will be an overestimate. A second possibility uses the creep strains in the element AC. Now $\varepsilon_c = 0$ at $\theta = \theta_o$, and its final value ε_c^* is such that an imperfection $(\varepsilon_i + \varepsilon_c^*)$ causes elastic buckling at the applied load P. The initial and final values $\dot{\varepsilon}_{co}$ and $\dot{\varepsilon}_c^*$ of $\dot{\varepsilon}_c$ may also be found from the stress in AC calculated using elastic analyses at these conditions. Now $\dot{\varepsilon}_c$ is known to be an increasing function of θ and t, so

$$(\varepsilon_c^*/\dot{\varepsilon}_c^*) < t^* < (\varepsilon_c^*/\dot{\varepsilon}_{co}). \qquad (13)$$

In most cases these upper and lower bounds on t^* are not at all close, but they tend to be better in precisely the situations when ordinary small deflection analyses are inadequate and some kind of large deflection treatment is needed.

6. Conclusions

The analyses of sections 3 and 4 seem to indicate that the instantaneous buckling behaviour of a structure is reflected in its creep response. If the instantaneous post-buckling is stable then true creep buckling with infinite displacement rate does not in fact occur, though large displacements may limit the structure's useful life. A small deflection analysis then appears to be safe in that it overestimates deflections at all times. If the postbuckling is unstable then an infinite deflection rate develops at finite deflection and finite critical time, when the system encounters the instantaneous critical point locus. A small deflection analysis is then unsafe in that it underestimates deflections and over-estimates the critical time. These observations may be relevant, for example, to cylindrical shells, which sometimes have very unstable postbuckling.

The small deflection analysis approximations are negligible if conditions (a) to (c) of section 3.1 are satisfied. Most metallic materials have $n > 2$, so that (a) is satisfied. Such analyses are unsafe only for structures with unstable postbuckling, and for these structures considerations of safety relating to the effects of imperfection sensitivity on the instantaneous response are likely to ensure that (b) and (c) are satisfied in practice.

Finally it must be realised that these ideas have been developed in the context of single degree of freedom systems. Practical structures tend to have infinite degrees of freedom, but frequently the buckling phenomenon is essentially confined to a single buckling mode. This is reflected in Hoff's neglect of all displacement terms other than that for the first mode in many of his analyses. Thus it is hoped that the present work may be relevant to real structures.

References

(1) HOFF, N.J., "Buckling and stability", J. Roy. Aero. Soc. 58, no. 517 (1954).

(2) HULT, J.A.H., "Creep buckling of plane frameworks", Trans. Royal Institute of Technology, Stockholm, Mech. Engng. 1, 136 (1959).

(3) HOFF, N.J., "Creep buckling", Aeronautical Quarterly 7 (1956).

(4) PATEL, S.A., "Buckling of columns in the presence of creep", ibid.

(5) CHAPMAN, J.C., ERICKSON, B. and HOFF, N.J., "A theoretical and experimental investigation of creep buckling", Int. J. Mech. Sci. 1 (1960).

(6) HOFF, N.J., "Creep buckling of rectangular plates under uniaxial compression", Engineering Plasticity, ed. J. Heyman and F.A. Leckie, Cambridge University Press, Cambridge, England (1968).

(7) HOFF, N.J., "Axially symmetric creep buckling of circular cylindrical shells in axial compression", J. Appl. Mech. 35, Series E, No. 3(1968).

(8) SAMUELSON, L.Å., "Creep buckling of a circular cylindrical shell", A.I.A.A. Journal 7 (1960).

(9) SAMUELSON, L.Å., "Creep buckling of a cylindrical shell under non-uniform loads", Int. J. Solids Structures 6 (1970).

(10) HOFF, N.J., "Creep buckling of plates and shells", Stanford University, Dept. of Aeronautics and Astronautics Report SUDAAR No. 443 (1972).

(11) CROLL, J.G. and WALKER, A.C., Elements of Structural Stability, Macmillan, London, England (1972).

(12) THOMPSON, J.M.T. "A general theory for the equilibrium and stability of discrete conservative systems", Z. Angew. Math. Phys. 20 (1969).

(13) THOMPSON, J.M.T., "Discrete branching points in the general theory of elastic stability", J. Mech. Phys. Solids 13 (1965).

Table I. Computed response of first link model with $\theta_i > 0$.

n	$\frac{P}{P_e}$	θ_i	Large deflection analysis			Small deflection analysis	
			θ^*	$\left(\frac{E}{\lambda}\right)^n t^*$	$\left(\frac{E}{\lambda}\right)^n t_{0.2}$	$\left(\frac{E}{\lambda}\right)^n t^*$	$\left(\frac{E}{\lambda}\right)^n t_{0.2}$
1	0.1	0.0001	0.9520	72.1	65.4	∞	67.4
		0.001	"	51.4	44.7	"	46.7
		0.01	"	30.8	24.0	"	26.1
		0.1	"	10.98	4.3	"	5.3
	0.5	0.0001	0.4026	6.61	6.41	"	6.91
		0.001	"	4.31	4.11	"	4.61
		0.01	"	2.04	1.84	"	2.30
		0.1	"	0.0570	0	"	0
	0.9	0.0001	0.0690	0.360	(0.360)	"	0.589
		0.001	"	0.1121	(0.1121)	"	0.333
		0.003	"	0.01039	(0.01039)	"	0.211
3	0.1	0.0001	0.9520	1.457×10^{11}	1.457×10^{11}	1.458×10^{11}	1.458×10^{11}
		0.001	"	1.451×10^{9}	1.451×10^{9}	1.458×10^{9}	1.458×10^{9}
		0.01	"	1.387×10^{7}	1.386×10^{7}	1.458×10^{7}	1.454×10^{7}
		0.1	"	0.899×10^{5}	0.70×10^{5}	1.458×10^{5}	1.01×10^{5}
	0.5	0.0001	0.4026	1.997×10^{8}	1.997×10^{8}	2.000×10^{8}	2.000×10^{8}
		0.001	"	1.996×10^{6}	1.965×10^{6}	2.000×10^{6}	2.000×10^{6}
		0.01	"	1.676×10^{4}	1.672×10^{4}	2.000×10^{4}	1.980×10^{4}
		0.1	"	6.486	0	2.000×10^{2}	0
	0.9	0.0001	0.0690	2.622×10^{5}	(2.622×10^{5})	2.743×10^{5}	2.743×10^{5}
		0.001	"	1.638×10^{3}	(1.638×10^{3})	2.743×10^{3}	2.737×10^{3}
		0.003	"	1.933×10	(1.933×10)	3.048×10^{2}	2.98×10^{2}

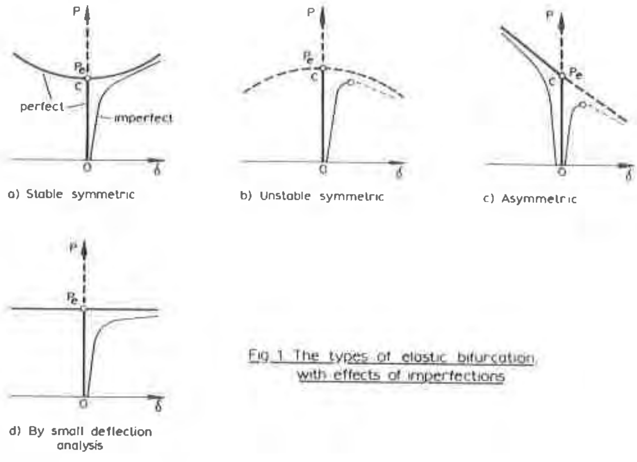

Fig. 1 The types of elastic bifurcation with effects of imperfections

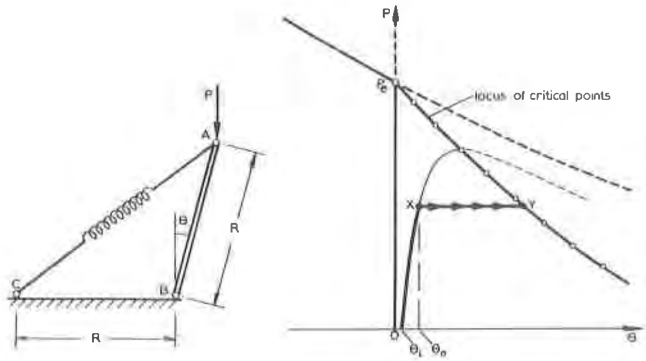

(a) (b)

Fig. 2. The first link model and its response

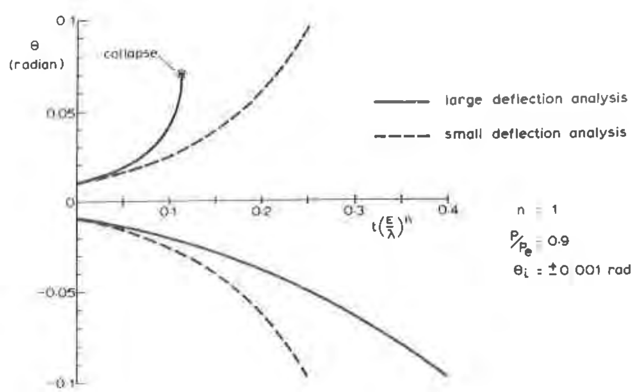

Fig. 3. Displacement - time curves for first link model

Fig. 4. The second link model

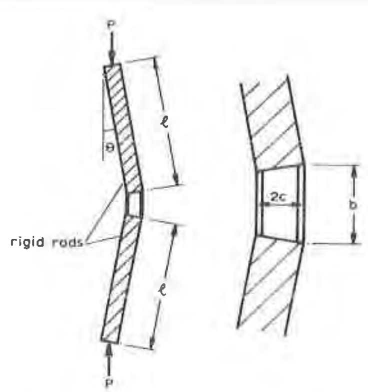

Fig. 5. The Shanley column model with enlarged view of central cell